Spin transport in lateral ferromagnetic/nonmagnetic hybrid structures

2007 J. Phys.: Condens. Matter 19 165216

(http://iopscience.iop.org/0953-8984/19/16/165216)

IOP PUBLISHING JOURNAL OF PHYSICS: CONDENSED MATTER

J. Phys.: Condens. Matter **19** (2007) 165216 (13pp) doi:10.1088/0953-8984/19/16/165216

Spin transport in lateral ferromagnetic/nonmagnetic hybrid structures

T Kimura and Y Otani

Institute for Solid State Physics, University of Tokyo, 5-1-5 Kashiwanoha, Kashiwa, Chiba 277-8581, Japan
and
RIKEN FRS, 2-1 Hirosawa, Wako, Saitama 351-0198, Japan

E-mail: kimura@issp.u-tokyo.ac.jp

Received 26 June 2006, in final form 12 September 2006
Published 6 April 2007
Online at stacks.iop.org/JPhysCM/19/165216

Abstract

Laterally configured ferromagnetic/nonmagnetic multi-terminal spintronic devices enable the performance of detailed study of spin accumulation in nonmagnets. The spin diffusion processes in lateral structures are investigated using nonlocal spin injection techniques. Efficient spin injection and detection are accomplished by optimizing the probe configuration and junction structures on the basis of the concept of spin resistance. The magnetization switching of a nanoscale ferromagnet is finally realized using efficient spin current absorption behaviour induced by nonlocal spin injection.

(Some figures in this article are in colour only in the electronic version)

1. Introduction

Ferromagnet (F)/normal metal (N) hybrid systems show intriguing properties in association with spin transfer and accumulation. Such spintronic devices have great advantages over conventional electronic devices because of additional spin functionalities [1]. To realize these devices, electrical spin injection from F into N, semiconductor or superconductor is a key technique [2]. Therefore, understanding the physics responsible for the spin injection and diffusion processes is indispensable for the development of spintronic devices.

When a spin-polarized current flows across the junction between F and N, chemical potential splitting is induced in the N layer because of a sudden change in spin-dependent electrical conductivity [3]. This leads to spin accumulation in the vicinity of the F/N interface. The injected spin can be flipped due to spin–orbit interaction, magnon or phonon scattering, etc. The length scale over which the travelling electron spin memorizes the initial direction is known as the spin diffusion length, an important measure for realizing efficient spin injection.

In order to study the spin diffusion process, most experiments have been carried out in a vertical structure called the current perpendicular to plane (CPP) configuration [4]. It is,

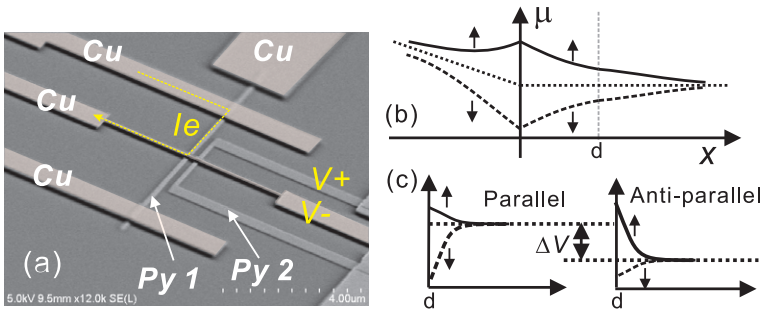

Figure 1. (a) SEM image of a fabricated lateral spin-valve device consisting of two permalloy (Py) wires bridged by a Cu strip. (b) Schematic illustration of the chemical potential of the Cu strip under spin injection from a Py wire. (c) Schematic illustration of the chemical potential in the Py voltage probe.

however, difficult to fabricate multi-terminal devices with vertical structures, so one can only obtain limited information about the series resistance of the magnetic multilayers. On the contrary, laterally configured F/N hybrid devices have great potential for the development of a new class of spintronic devices such as a spin transistors [5], spin batteries [6], etc. However, it has been difficult to detect spin-dependent signals in lateral structures because the spurious magnetoresistance effects such as anisotropic magnetoresistance and the anomalous Hall effect smear the intrinsic signals. Nonlocal spin injection, by which the spin and charge currents are well separated, is a powerful means for detecting the spin-dependent signals in lateral structures because irrelevant magnetoresistance changes can be removed [7]. In this paper we discuss the spin diffusion process in lateral F/N hybrid structures using nonlocal spin injection to develop efficient methods for spin injection and accumulation.

2. Detection of spin accumulation by mean of nonlocal spin injection

We apply a nonlocal spin-valve (NLSV) measurement to our lateral spin-valve (LSV). LSV devices are fabricated by means of electron beam lithography and a lift-off technique. Figure 1(a) shows a scanning electron microscope (SEM) image of a typical LSV consisting of two Permalloy (Py) wires bridged by a Cu wire. First, we fabricated two Py wires 120 nm wide and 30 nm thick. The Py wires were grown by an electron beam evaporator with a base pressure of 2×10^{-9} Torr. The centre–centre distance between the Py wires is 270 nm. Then, an 80 nm thick Cu wire was formed across the Py wires by a resistance heating evaporator with a base pressure of 3×10^{-8} Torr. The interface between the Py and the Cu wires was carefully cleaned by low voltage Ar-ion milling prior to the Cu deposition. The contact resistance of the interface was ohmic and very low, indicating a transparent contact. The resistivities of Py and Cu wires, respectively, are 26.8 and 2.08 $\mu\Omega$ cm at room temperature. Here, one Py wire has large pads connected to its edges to facilitate domain wall nucleation, while the other one has flat-end edges. We can thus control the magnetization configuration (parallel or anti-parallel) by adjusting the magnetic field. Nonlocal resistance measurements were performed using a standard current-bias lock-in technique with the external magnetic field parallel to the Py wires.

As shown in figure 1(a), the electric current is injected from the Py into the left-hand side of the Cu wire. Then, the spin accumulation is induced not only in the left-hand side of the Cu but also in the right-hand side of the Cu as shown in figure 1(b). When one attaches another

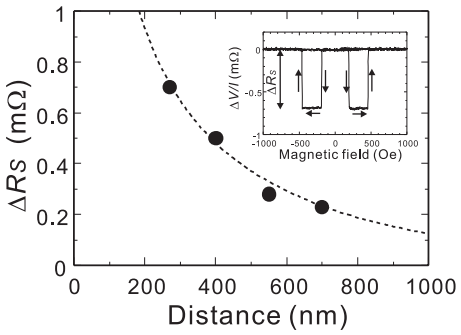

Figure 2. Nonlocal spin-valve signal as a function of the electrode distance between two Py wires. The inset shows the nonlocal spin-valve signal curve at a distance of 270 nm measured at room temperature.

ferromagnet Py2 to the right-hand side of the Cu, the spin splitting of the chemical potential is induced also in Py2 because of the continuity of the chemical potential at the interface. The neutral point for chemical potential in Py2 shifts from the middle point because of the spin-dependent conductivity. Therefore, the voltage difference is induced between Py2 and the right-hand side of the Cu wires as shown in figures 1(b) and (c). Figure 2(a) shows the field dependence of the NLSV signal measured at room temperature. The NLSV curve exhibits a clear spin-valve signal corresponding to either a parallel (high) or anti-parallel (low) state as in figure 2(a). The resistance change due to spin accumulation, ΔR_S, is 0.7 mΩ at room temperature.

We then experimentally estimate the spin diffusion lengths of Py strips (λ_{Py}) and Cu strips (λ_{Cu}), and the spin polarization of Py strips (α_{Py}). The distance between the injector and detector junctions is varied from 270 to 700 nm and we measure the NLSV signal at room temperature as a function of this distance. The obtained signal decreases monotonically with increasing distance d because of spin relaxation. From the one-dimensional spin-diffusion model, the induced spin valve signal can be calculated by [8, 9]

$$\Delta R_S = \frac{\alpha_{Py}^2 Q^2 R_{SCu}}{2e^{(d/\lambda_{Cu})}\, Q(2+Q) + 4\sinh(d/\lambda_{Cu})} \tag{1}$$

where R_{SCu} and R_{SPy} are the spin resistances of Cu and Py, respectively. The spin resistance, which is defined as $2\lambda/((1-\alpha^2)(\sigma S))$ with effective cross sectional area S, spin polarization α, conductivity σ and spin diffusion length λ, is a measure of the difficulty of spin mixing, and is comparable to the characteristic impedance for the spin current and spin-splitting voltage with the attenuation constant λ. To calculate the spin resistance, we have to carefully estimate the cross sections. λ_{Cu} is of the order of several hundred nanometres and λ_{Py} is a few nanometres [7, 12, 11, 10]. Since the spin current flows along the Cu strip over a few hundred nanometres the area S_{Cu} for estimating R_{Cu} should be given by the cross section of the Cu strip, in the present case 100 nm $\times$ 80 nm. On the other hand, in the Py strip the cross section is not appropriate for the area S_{Py} for R_{SPy} because the spin current diminishes in the vicinity of the junction. Therefore, for the Py strip S_{Py} should be the junction area, in the present case 100 nm $\times$ 100 nm [8, 9]. As shown in the figure 3(b), the fitted curve is in good agreement with the experimental results. From the fitting parameter, we obtain the spin-diffusion length of the Cu strip and that of the Py strip as 500 and 3 nm, respectively. The polarization α_{Py} of the Py strip is determined as 0.25 at room temperature. Here, $\lambda_{Cu} = 500$ nm is quite long compared with other reported values [7, 11]. We notice that the resistivity of our Cu is rather smaller

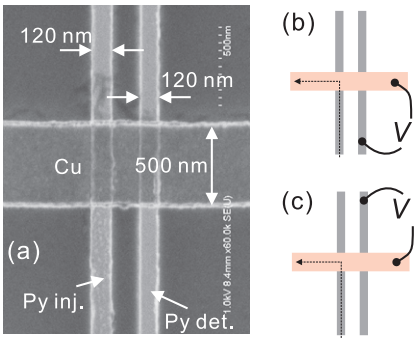

Figure 3. (a) SEM image of the fabricated lateral spin device. The NLSV probe configurations of (b) 'Half' and (c) 'Cross'.

than that of the reported one. This supports the long spin diffusion length of our Cu strip. The $\lambda_{Py} = 3$ nm and $\alpha_{Py} = 0.25$ are reasonable, although the values are slightly smaller than other group's values. This may be due to the rather higher resistivity of our Py than others. Using these values, we can calculate the characteristic spin resistance of each strip as $R_{SCu} = 2.60\ \Omega$ and $R_{SPy} = 0.34\ \Omega$. The spin current flows preferentially in the Py wire. This means that the induced spin current prefers to flow in the Py wire rather than to the Cu wire. As mentioned later, additional contacts with Py strongly modify the total spin resistance in the system.

3. Geometrical effect in spin accumulation

Understanding the spatial distributions of the spin current and spin accumulation are essential for the development of spintronic devices. So far, most studies on the spin injection have been carried out using a one-dimensional diffusive model [7, 3, 8, 2, 13]. However, in realistic cases, two-dimensional spin diffusion cannot be neglected. In this section, we show the geometrical effect on the spin signal [14] and the importance of the probe configuration for obtaining an efficient spin signal [16].

Figure 3(a) shows a SEM image for the LSV fabricated for this study. Here, the width of the Cu wire is 500 nm. We measured the nonlocal spin-valve signal in two different probe configurations. One is the configuration where the current and voltage probes are located on the same side of the Ni–Fe wires with respect to the Cu wire, say 'Half', as shown in figure 3(b). The other is the one where the current and the voltage probes are diagonally placed, say 'Cross', as shown in figure 3(c).

Figure 4(a) shows NLSV curves at the Half probe configuration. The obtained spin-valve signal is 0.58 mΩ. On the other hand, the NLSV signal in the Cross configuration is 0.12 mΩ, and is much smaller than that in the Half configuration, as shown in figure 4(b). Needless to say, in a one-dimensional model, the obtained signal should be the same [7, 8, 13]. Thus, in order to understand this deviation, we have to consider the spatial distribution of the spin current. Figure 4(c) shows the spatial distribution of the spin current density inside Cu at a depth of −5 nm from the Py/Cu interface plane, calculated by a 3D network of the spin-polarization-dependent elements [15]. The spin current distribution in the vicinity of Py-inj/Cu and Py-det/Cu interfaces is very inhomogeneous. This is partly due to the large difference in conductivity between Cu and Py, and partly due to the very small spin diffusion length of Py. In particular, most of the spin current is injected in the vicinity of the bottom edge of the NiFe-inj/Cu interface. Consequently, the effective distance between the spin injector and detector is

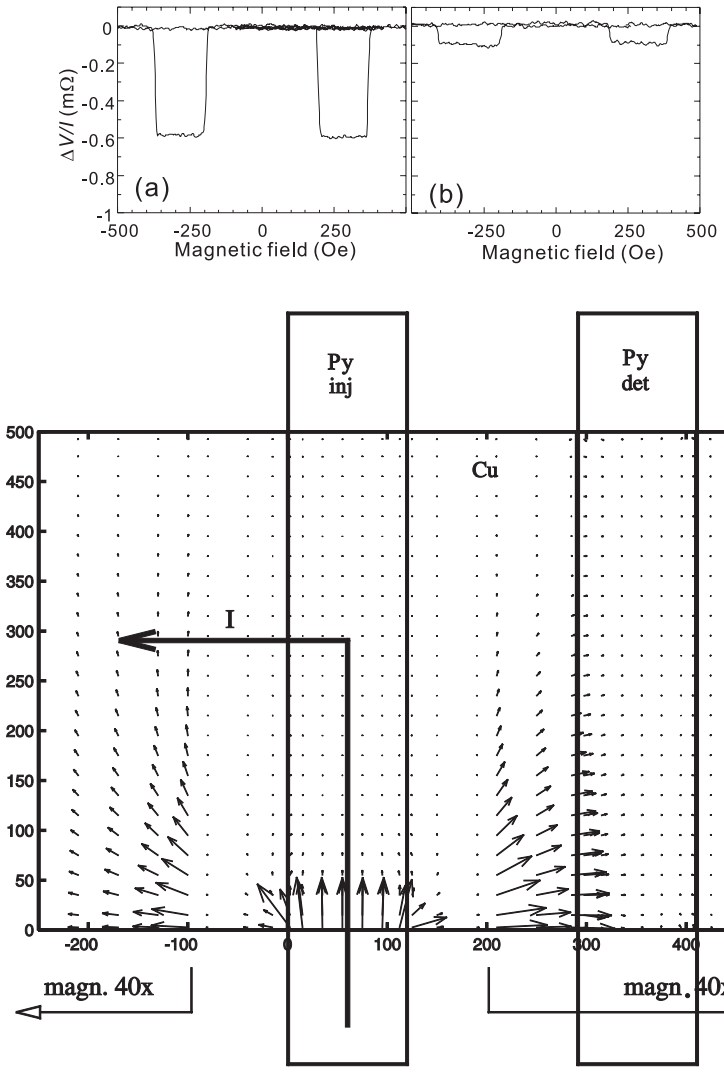

Figure 4. Nonlocal spin-valve curves in (a) Half and (b) Cross configurations measured at room temperature. (c) Calculated spatial distribution of the spin current density inside the structure. The direction and the length of the arrow at each segment correspond to the direction and the magnitude of the spin current. The lengths of the arrows in the regions $x < 100$ nm and $x > 200$ nm have been magnified $40\times$ with respect to the central part including the injector.

shorter for the Half than for the Cross configuration. Therefore, a smaller spin-valve signal is expected for the Cross configuration.

Using this inhomogeneity, we can detect the spin accumulation signal with an another probe configuration. The electrochemical potential varies in order to ensure the continuity of the chemical potential over the whole interface between the F and N strips whereby the spin-polarized current flows in the F strip. Therefore the detectable voltage drop, the direction of which depends on the magnetic orientations between the F injector and the detector strips, will appear along the F strip. We measured the induced voltage drop across the Cu strip along the F detector under nonlocal spin injection, as shown in figure 5(a). This probe configuration is

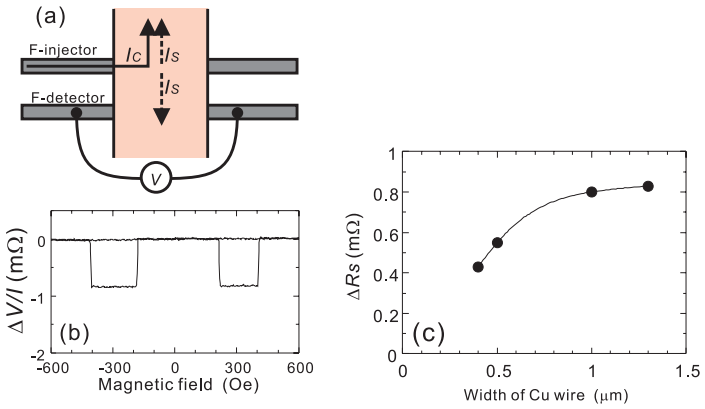

Figure 5. (a) Schematic illustration of conventional nonlocal spin-valve devices. Based on the one-dimensional model, the spin current along the Cu wire is induced in the nonlocal lead. (b) Nonlocal transverse spin signals measured at 77 K with a Cu width of 1.3 μm. (c) The NLTS signal changes as a function of the width of the Cu wire.

similar to that for measurement of the nonlocal Hall resistance (NLHR) because the voltage is induced transverse to the current in one-dimensional systems [18, 17]. In conventional NLSV measurements, the detected voltage difference between N and F strips is caused by the boundary resistance between the F/N interface [7–9, 20]. However, in the present probe configuration, the detected signal does not include any boundary resistance.

Figure 5(b) shows the result for the NLTS signal measured at 77 K, exhibiting a clear spin-dependent effect with a magnitude of 0.82 mΩ. This behaviour is quite similar to that of the NLSV signal, although the measured resistance does not include any boundary resistance at the F/N interface. As mentioned above, the spin-dependent signal in this configuration is caused by the change in the direction of the induced current corresponding to the magnetization direction. In this way, a spin-polarized current can be effectively induced along the F strip.

The induced NLTS should decrease on reducing the width w of the Cu wire because of the reduction of the inhomogeneity. Figure 5(c) shows the dependence of the NLTS signal on the width of the Cu wire. As we expect, the NLTS signal increases with increasing wire width. However, it saturates when $w > 1.0$ μm. This means that spin accumulation diminishes at the right-hand edge of the F/N junction at $w > 1.0$ μm because the diagonal distance from the current injecting point to right-hand edge becomes longer than the spin-diffusion length of the Cu wire [9].

4. Efficient spin accumulation with local spin injection

Obtaining a large magnetoresistance or spin signal by spin injection is one of the main issues for realizing spintronic devices. Local configuration induces a spin accumulation two times larger than that in the nonlocal configuration. However, the detected signal includes the large background resistance of the Cu ohmic resistance and is known to be dominated by the anistropic magnetoresistance (AMR) from the ferromagnetic electrodes [7]. We can reduce such contributions by using the narrow ferromagnetic wires and thick Cu wire [19]. Figure 6(b) shows the change in magnetoresistance in the local probe configuration shown in figure 6(a). The resistance change exhibits a clear spin-valve signal without any spurious signal from the ferromagnetic wire. The obtained spin-valve signal is 4 mΩ, about two times larger than that of NLSV.

We now demonstrate efficient nonlocal spin injection combined with local spin injection [20]. In the local configuration, the induced splitting of the chemical potential in

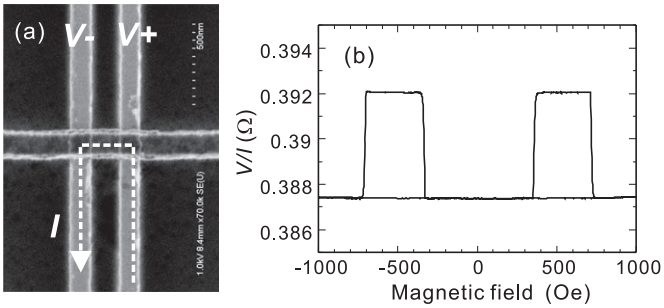

Figure 6. (a) SEM image of the fabricated LSV with the probe configuration for the local spin valve measurement. (b) Local spin-valve curve measured at 77 K.

the N in the anti-parallel configuration is larger than that in the parallel configuration, as shown in figure 7(a) [19]. To maintain the continuity of the chemical potential in the N layer, a large spin splitting can be induced both in the local nonmagnetic region with the charge current and in the nonlocal region without the charge current. We can thus expect a much larger spin signal than for a conventional NLSV measurement once the NLSV is combined with the above mentioned local current injection. To realize this idea, we fabricated a lateral spin injection device consisting of three ferromagnetic wires bridged by a Cu wire, shown in figure 7(b). There are three Py wires of different width, denoted as Py1, Py2 and Py3. To obtain different switching fields among the Py wires, the widths and edge shapes are designed appropriately as follows. The widths of Py1, Py2 and Py3 are 180, 80 and 120 nm, respectively. Py3 is connected to the large pad while Py1 and Py2 have flat ends. This results in the smallest switching field for the Py3 wire. The thickness of the Py wires is 30 nm. The spacing between each Py wire is 200 nm. The dimensions of the Cu wire are width 250 nm and thickness 80 nm. The switching fields of the Py1, Py2 and Py3 wires were found 400, 450 and 200 Oe, respectively. The magnetic orientation of the Py wires can thus be controlled by setting the magnetic field between different switching fields of three Py wires.

We performed a NLSV measurement with local current injection in either the parallel or anti-parallel configuration as follows. The current flows from wire Py1 to Py2 and the voltage difference between wires Py2 and Py3 was measured, as shown in the inset of figures 7(c) and (d). Before starting the measurement, the orientation of the magnetization between Py1 and Py2 was set either in the parallel or the anti-parallel state. We then swept the magnetic field between -300 and 300 Oe, meaning that the magnetization directions of Py1 and Py2 are fixed while the magnetization of Py3 is switched during the measurements. Figures 3(a) and (b) show the NLSV minor loops measured with Py1 and Py2 parallel and anti-parallel, respectively. As explained above, we can induce a large spin polarization in the nonmagnetic layer when the local current injection is performed with Py1 and Py2 in the anti-parallel configuration. As shown in figure 3, the obtained spin signal in the anti-parallel configuration increases to 1.9 mΩ whereas that in the parallel configuration is 1.3 mΩ. Thus, the spin signal in the NLSV configuration can be increased by changing the magnetization configuration for the local spin current injection.

5. Influence of an additional ohmic contact

In the NLSV measurement, a ferromagnetic wire is used to detect the spin accumulation in the N. However, we have to note that the ferromagnet with a small spin resistance connected to the N significantly affects the distribution of the spin-dependent electrochemical potential in

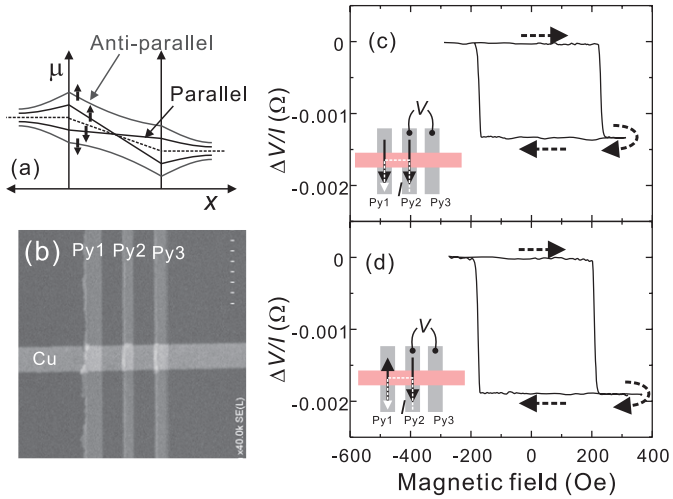

Figure 7. (a) Spatial distribution of the spin-dependent chemical potential in the nonmagnetic layer in the parallel and anti-parallel state for local current injection. (b) SEM images of the fabricated lateral spin device consisting of three Py wires bridged by a Cu wire. Minor loops of nonlocal spin-valve measurements with local current injection (c) in the parallel state and (d) in the anti-parallel state. The insets shows the probe configuration for the measurement and the magnetization orientation.

the N because the spin current is preferably absorbed and equilibrated in the F. In this section, we demonstrate the spin absorption effect using a lateral spin-valve device consisting of three ferromagnetic wires bridged by a Cu strip [21].

The suppression of the spin accumulation can be demonstrated by the NLSV measurement using the LSV consisting of three Py wires with the probe configuration shown in the inset of figure 8(a). As mentioned above, the Py connected to the Cu reduces the spin splitting of the chemical potential in the Cu and spin-valve signal. Therefore, when we perform the NLSV measurement with the Py1 and Py3 wires, the spin-valve signal is expected to be much smaller than the conventional NLSV signal. Figure 8(a) shows that the obtained small NLSV signal of 0.04 mΩ coincides well with the above expectation. The geometrical disorder due to the additional ferromagnetic contact may also violate the spin coherence and the spin accumulation. However, we believe that such an effect is negligible because of the large difference in thickness between Cu and Py.

For comparison, we also fabricated a lateral spin-valve consisting of two Py wires separated by 600 nm, longer than the 460 nm spacing between Py1 and Py3 in figure 8(a). The thickness and the width of the Py and Cu wires are the same as those of the previous spin-valve device consisting of three Py wires. The SEM image of the fabricated device is shown in the inset of figure 8(b). If there is no suppression due to an additional ferromagnetic wire in the previous experiment, the NLSV signal of this sample should be at least smaller by a factor of about 0.7 than that of figure 8(a). Figure 8(b) shows the NLSV signal measured in the probe configuration shown in the inset of figure 8(b). The obtained spin signal is 0.2 mΩ, much larger than that of figure 8(a). These results clearly support that spin accumulation in the N is suppressed by the ferromagnetic wire connected to the N. We note here that in the spin signal with the middle Py wire insertion no change is observed at the switching field of the middle wire. This means that the magnitude of the spin current absorption does not depend on the magnetization configuration of the middle wire.

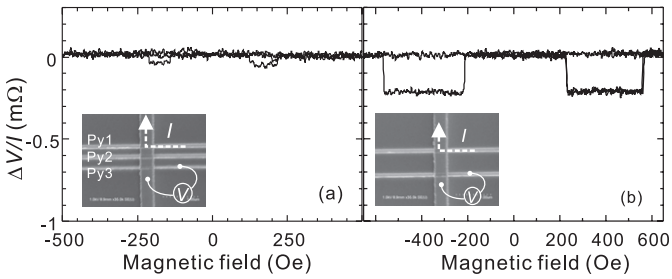

Figure 8. (a) Nonlocal spin-valve signal for a lateral spin-valve consisting of three Py wires with the middle Py wire insertion. The inset shows an SEM image of the device and the probe configuration for the measurement. (b) Nonlocal spin-valve signal for a lateral spin valve consisting of two Py wires with a spacing 600 nm. The inset shows the SEM image of the device and the probe configuration for the measurement.

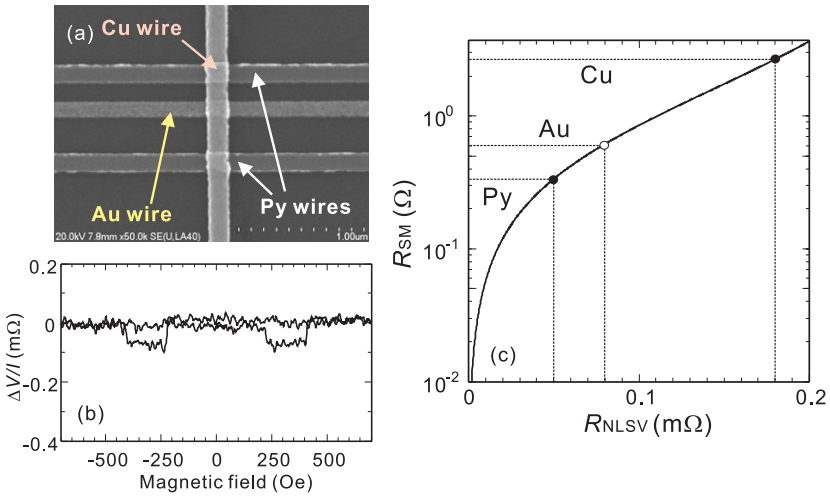

Figure 9. (a) SEM images of a typical lateral spin device consisting of double Py/Cu junctions and a middle Au/Cu junction. (b) Nonlocal spin-valve curve with Au middle insertions, (c) Calculated spin resistance as a function of the obtained nonlocal spin signal R_{NLSV}.

The spin accumulation is also suppressed by connecting the nonmagnetic wire to a small spin resistance. We prepare the lateral spin-valves consisting of triple junctions by changing the material for the middle (M) strip. Figure 9(a) shows the NLSV signal of the device with an Au M strip. The obtained spin signal is 0.08 mΩ and shows a large reduction of the spin signal similar to that of a Py M strip. This implies that the Au wire has a smaller spin resistance.

The spin signal ΔR_{S} can be calculated as the following equation with the spin resistance of R_{SM} of the middle strip [9]:

$$\Delta R_{\mathrm{S}} \approx \frac{\alpha_F^2 Q^2 Q_{\mathrm{M}} R_{\mathrm{SN}}}{2\left(-2+2\cosh\left(\frac{d}{\lambda_{\mathrm{N}}}\right)+2Q_{\mathrm{M}}\sinh\left(\frac{d}{\lambda_{\mathrm{N}}}\right)\right)}. \tag{2}$$

We know the spin resistances of Py and Cu strips from the previous double-junction experiment Therefore, we obtain the following relation between the detected spin signal R_{NLSV} and R_{SM}

$$R_{\mathrm{SM}}\ (\Omega) = \frac{7.02 R_{\mathrm{NLSV}}\ (\mathrm{m}\Omega)}{1.27 - 4.41 R_{\mathrm{NLSV}}\ (\mathrm{m}\Omega)}. \tag{3}$$

This means that the spin resistance and the spin diffusion length of the middle strip can be estimated from the magnitude of the spin signal. In this calculation, the spin signal with the middle wire insertion does not depend on the magnetization configuration of the middle wire.

Figure 9(b) shows the spin resistance of the M strip R_{SM} as a function of R_{NLSV} based on equation (3). From the equation, we obtain the spin resistances of the Cu, Au and Py strip as 2.67, 0.62 and 0.33 Ω. The experimental values for the Py and Cu M strips are quantitatively in good agreement with the ones obtained from the double junction experiment. This indicates that equation (3) is valid for estimating the spin resistance of the M strip. For the Au strip, since the resistivity of the Au strip is 5.24 $\mu\Omega$ cm, we obtain the spin-diffusion length of the Au strip as 60 nm. This is in good agreement with the other reports [12] and proves that the Au strip has a short spin-diffusion length due to the strong spin–orbit interaction [22]. Thus, using this method, we can estimate the characteristic spin resistance and spin diffusion length of the material.

6. Efficient spin accumulation by reducing junction size

As mentioned above, the inhomogeneous current distribution in the vicinity of the ohmic junction affects the spin signal in lateral structures [14]. The spatial distribution of the spin current and accumulation can be well calculated by the spin resistance circuit model [9]. From the calculation, the spin accumulation and current are found to depend not only on the electrode spacing but also on the spin resistance of each constituent segment. Therefore, the spin polarization induced in the Ns should depend on the F/N junction size. In this section, we experimentally demonstrate that the size of the ohmic F/N junction is an important geometrical factor for obtaining large spin polarization in Ns and that both the spin polarization and the spin resistance of the F are enhanced by adjusting the junction size [23].

The device geometry is quite similar to that of the device used in [7]. As mentioned above, the difference in the junction size between injector and detector gives rise to a significant difference in the spin resistance. We calculate the spin signal induced in the asymmetric LSV using our previous spin-resistance circuit model. In the cross-shaped Cu wire, the effective spin resistances of the vertical Cu arms are much smaller than the horizontal Cu arms because the vertical Cu arms have additional ohmic contacts with the Py pad and wire [9]. Therefore, in the calculation we neglect the influence of the horizontal Cu arms. The spin signal of the NLSV measurement can be calculated as

$$\Delta R \approx \frac{\alpha_{Py}^2 R_{SPy}^P R_{SPy}^W}{R_{SCu} \sinh\left(\frac{d}{\lambda_{Cu}}\right)}. \tag{4}$$

Here, R_{SPy}^P, R_{SPy}^W and R_{SCu} are, respectively, the spin resistances of the Py pad, the Py and Cu wires. α_{Py}, λ_{Cu} and d are, respectively, the spin polarization of the Py, the spin diffusion length of the Cu wire and the average travelling length for the electron spin from the injector to the detector.

As mentioned above, reducing the size of the ohmic junction between the Py pad and the Cu wire increases the spin resistance of the Py pad. The size of the junction area can be reduced by cutting the Cu wire on the Py pad, as seen in the inset of figure 10. We change the size of the Py/Cu junction while keeping the same electrode spacing of 600 nm and study the dependence of the spin signal on the junction size. The spin signal is plotted as a function of the junction size in figure 10. The spin signal increases with reduction of the junction size and is well reproduced by equation (4), where the spin signal is inversely proportional to the junction size. From the fitting parameters, we obtain the spin resistances of the Cu wire and the Py wire as

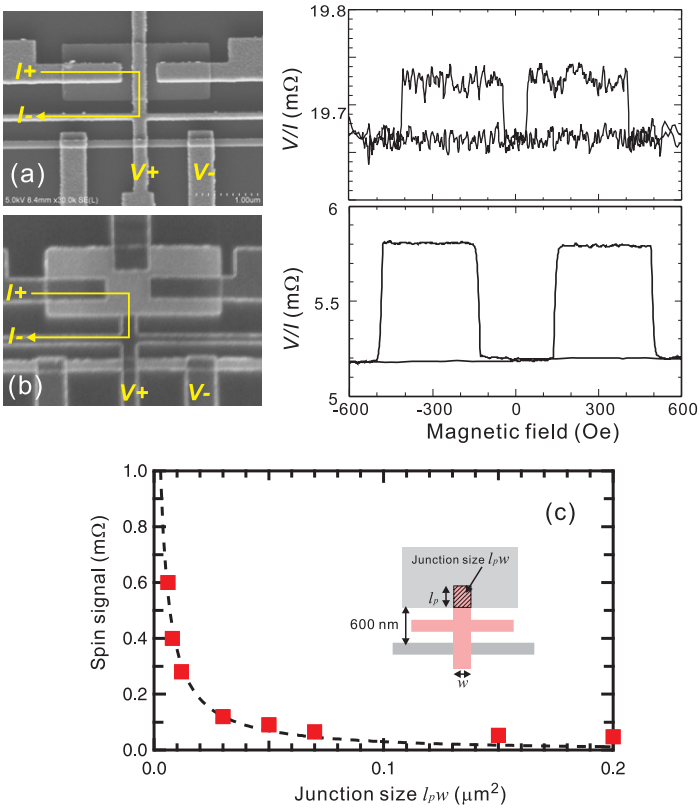

Figure 10. Nonlocal spin valve signals of (a) the large-junction device and (b) the small-junction device with the probe configurations. (c) Spin signal in the NLSV measurement as a function of the junction size $l_p w$. The dotted curve is the best fitting to the data points using equation (4).

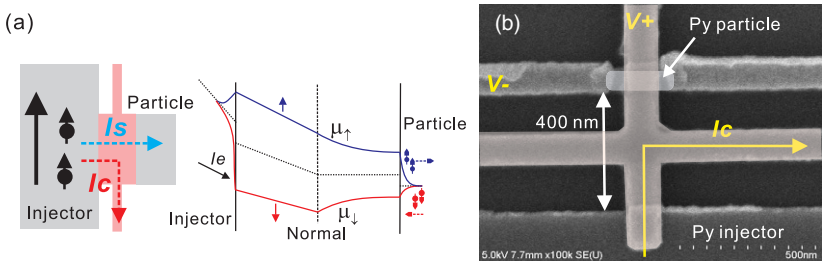

Figure 11. (a) Schematic illustration of nonlocal spin injection using lateral spin-valve geometry. Only spin current is injected into the small ferromagnetic particle. (b) Scanning electron microscope image of the fabricated lateral spin-valve. The device consists of a large 30 nm thick Py injector, a Cu cross 100 nm wide and 80 nm thick, and a Py nanoscale particle, 50 nm wide, 180 nm long and 6 nm thick.

2.14 and 0.08 Ω, respectively. The spin diffusion length of the Cu wire is found to be 1.5 μm at 77 K, longer than the values in [7, 11]. This indicates that our Cu wire has a better quality than others. The spin polarization and the spin diffusion length of the Py wire are respectively 0.25 and 3.5 nm, reasonable values compared with previous experiments [7, 9, 10].

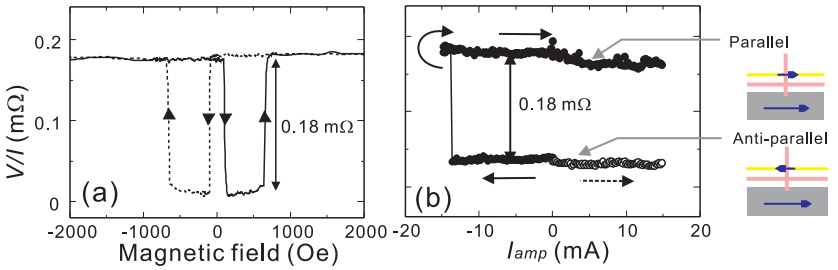

Figure 12. (a) Field dependence of the nonlocal spin signal. The changes in resistance at low and high fields correspond to the relative magnetic switching of the Py injector and particle, from parallel to anti-parallel states and vice versa. (b) Nonlocal spin-valve signal after the pulsed current injection as a function of the current amplitude with corresponding magnetization configurations.

7. Spin torque due to spin current absorption

The current-induced magnetization reversal becomes one of the key technologies for developing spintronic devices. The switching mechanism due to spin torque is explained with a model proposed by Slonczewski in which the torque exerted on the magnetization is proportional to the injected spin current. This clearly indicates that the spin current is essential for realizing magnetization switching due to the spin injection. Most of the present spin-transfer devices consist of vertical multilayered nanopillars in which typically two magnetic layers are separated by a nonmagnetic metal layer [24, 25]. In such vertical structures, the charge current always flows together with the spin current, thereby undesirable Joule heat is generated. We have demonstrated that the spin currents are effectively absorbed into an additionally connected metallic wire with a small spin resistance [9]. This implies that the spin current without a charge flow can be selectively injected into a ferromagnetic particle with a small spin resistance such as a Permalloy particle, replaced with the wire, and may contribute to the spin torque. To test this idea, a nanoscale ferromagnetic particle is configured for a lateral nonlocal spin injection device as in figures 11(a) and 11(b) [26].

The device consists of a large 30 nm thick Py, a Cu cross 100 nm wide and 80 nm thick and a Py nanoscale particle 50 nm wide, 180 nm long and 6 nm thick. A gold wire 100 nm wide and 40 nm thick is connected to the Py particle to reduce the effective spin resistance, resulting in high spin current absorption into the Py particle [9]. The magnetic field is applied along the easy axis of the Py particle. We note here that the dimensions of the Py pad and Cu wires are chosen large so that a charge current up to 15 mA can flow through them.

To confirm that the spin current from the Py injector is injected into the Py particle, nonlocal spin-valve measurements are performed. As in figure 12(a), the field dependence shows a clear spin-valve signal with a magnitude of 0.18 mΩ, ensuring that the spin current reaches the Py particle. Then, we examine the effect of nonlocal spin injection into the Py particle with using the same probe configuration. Before performing nonlocal spin injection, the magnetization configuration is set in the anti-parallel configuration by controlling the external magnetic field. Nonlocal spin injection is performed by applying large pulsed currents up to 15 mA in the absence of a magnetic field. As shown in figure 12(b), when the magnitude of the pulsed current is increased positively in the anti-parallel state, no signal change is observed up to 15 mA. On the other hand, for the negative scan, an abrupt signal change is observed at −14 mA. The change in resistance at −14 mA is 0.18 mΩ, corresponding to that of the transition from anti-parallel to parallel states. This means that the magnetization of the Py particle is switched only by the spin current induced by the nonlocal spin injection. The

spin current responsible for switching is estimated from the experiment to be about 200 mA, which is reasonable compared with the values obtained for conventional pillar structures.

8. Conclusion

We study the spin-diffusion processes in lateral spin-valve structures consisting of Py/Cu ohmic junctions. The results are well understood using an analysis based on spin-resistance circuits. We pointed out the two-dimensional distribution of the spin current and the importance of the probe configuration for the efficient detection of the spin accumulation. Efficient spin injection combined with a local spin injection is demonstrated. We also pointed out the importance of the size of the Py/Cu junction from the view point of the absorption of spin current, and finally demonstrated magnetization switching in the nonlocal configuration by using efficient spin current absorption.

References

[1] For example, Wolf S A, Awschalom D D, Buhrman R A, Daughton J M, von Molnar S, Roukes M L, Chtchelkanova A Y and Treger D M 2001 *Science* **294** 1488
[2] Schmidt G, Ferrand D, Molenkamp L W, Filip A T and van Wees B J 2000 *Phys. Rev.* B **62** R4790
[3] van Son P C, van Kempen H and Wyder P 1987 *Phys. Rev. Lett.* **58** 2271
[4] Pratt W P Jr, Lee S-F, Slaughter J M, Loloee R, Schroeder P A and Bass J 1991 *Phys. Rev. Lett.* **66** 3060
[5] Johnson M and Silsbee R H 1985 *Phys. Rev. Lett.* **55** 1790
[6] Brataas A, Tserkovnyak Y, Bauer G E W and Halperin B I 2002 *Phys. Rev.* B **66** 060404(R)
[7] Jedema F J, Filip A T and van Wees B J 2001 *Nature* **410** 345
Jedema F J, Nijboer M S, Filip A T and van Wees B J 2003 *Phys. Rev.* B **67** 085319
[8] Takahashi S and Maekawa S 2003 *Phys. Rev.* B **67** 052409
[9] Kimura T, Hamrle J and Otani Y 2005 *Phys. Rev.* B **72** 014461
[10] Dubois S, Piraux L, George J M, Ounadjela K, Duvail J L and Fert A 1999 *Phys. Rev.* B **60** 477
[11] Albert F J, Emley N C, Myers E B, Ralph D C and Buhrman R A 2002 *Phys. Rev. Lett.* **89** 226802
[12] Chiang W-C, Ritz C, Eid K, Loloee R, Pratt W P and Bass J 2004 *Phys. Rev.* B **69** 184405
[13] Fert A and Lee S 1996 *Phys. Rev.* B **53** 6554
[14] Kimura T, Hamrle J, Otani Y, Tsukagoshi K and Aoyagi Y 2005 *J. Magn. Magn. Mater.* **286** 88
[15] Hamrle J, Kimura T, Otani Y, Tsukagoshi K and Aoyagi Y 2005 *Phys. Rev.* B **71** 094402
[16] Kimura T, Hamrle J and Otani Y 2005 *J. Appl. Phys.* **97** 076102
[17] Takahashi S and Maekawa S 2002 *Phys. Rev. Lett.* **88** 116601
[18] Kimura T, Otani Y, Tsukagoshi K and Aoyagi Y 2004 *J. Magn. Magn. Mater.* **272–276** E1333
[19] Kimura T, Hamrle J, Otani Y, Tsukagoshi K and Aoyagi Y 2004 *Appl. Phys. Lett.* **85** 3501
[20] Kimura T, Hamrle J, Otani Y, Tsukagoshi K and Aoyagi Y 2004 *Appl. Phys. Lett.* **85** 5382
[21] Kimura T, Hamrle J, Otani Y, Tsukagoshi K and Aoyagi Y 2004 *Appl. Phys. Lett.* **85** 3795
[22] Pannetier B, Chaussy J, Rammal R and Gandit P 1985 *Phys. Rev.* B **31** R3209
[23] Kimura T, Otani Y and Hamrle J 2006 *Phys. Rev.* B **73** 132405
[24] Tsoi M, Jansen A G M, Bass J, Chiang W-C, Seck M, Tsoi V and Wyder P 1998 *Phys. Rev. Lett.* **80** 4281
[25] Albert F J, Emley N C, Myers E B, Ralph D C and Buhrman R A 2002 *Phys. Rev. Lett.* **89** 226802
[26] Kimura T, Otani Y and Hamrle J 2006 *Phys. Rev. Lett.* **96** 037201